Supporting information

S1. Experimental

S1.1 Synthesis of catalyst

$Ce_{0.15}Zr_{0.85}O_2$ solid solution was prepared by a modified co-precipitation route in a glass reactor (1L) equipped with a temperature-controlled chamber and four automatized pumps for adding reagents and controlling pH. Proper amounts of $Ce(NO_3)_3 \cdot 6H_2O$ salt (Treibacher Industrie AG) and $ZrO(NO_3)_2$ liquid gel (Treibacher Industrie AG) were dissolved in demineralised water obtaining a 0.2 M solution; concentrated H_2O_2 (35% Sigma-Aldrich) was then added according to the molar ratio $[H_2O_2]$/[tot metals ions] equal to 3. After 45min of continuous stirring at ambient temperature concentrated ammonium hydroxide (28% Sigma-Aldrich) was added to obtain a pH value of 10.5. Finally, lauric acid (Sigma-Aldrich), using a molar ratio ([tot metal ions]/[lauric acid]) equal to 0.25, was directly added in solid form to the reactor and maintained under continuous stirring for 4h. The precipitate was then filtered and washed three times with 0.5L of de-mineralized water and the resulting cake was dried at 100 °C overnight. The dry precipitate was calcined in air at 500 °C for 4h (fresh catalyst) followed by treatment at 1300 °C for 4h in N_2 flow (aged catalyst).

S1.2 Material Characterization

Surface area and porosity of the fresh catalyst were measured via isothermal N_2 adsorption/desorption technique using a Tristar 3000 gas adsorption analyzer (Micromeritics). Oxygen storage capacity (OSC) was measured by reducing the sample in 5 v% H_2/Ar flow at 650 °C for 1h, and by monitoring its weight loss via thermogravimetric analysis (Q500, TA Instruments). Temperature programmed reduction (TPR) was carried out in a 5 v%H_2 in He flow on 50mg fresh catalyst from room temperature up to 1100 °C (10 °C/min); the H_2 consumption was monitored by a TCD detector with a gas analyzer (Autochem 2100, Micromeritics).

Structural features of fresh and aged catalysts were investigated with X-ray diffraction technique (Philips PW3040/60 X'pert PRO instrument, Panalytical). Diffraction profiles were collected in the 20–145° 2θ range with a step of 0.02° and a counting time of 40s/step. The Rietveld analysis of X-ray profiles was carried out using the GSAS-EXPGUI program[1,2] to determine the compositions and amount of segregated components.

The surface composition and crystalline structure of the aged catalyst before and after testing were also investigated by X-Ray Photoelectron Spectroscopy (XPS) and High-Resolution Transmission Electron Microscopy (HRTEM).

XPS analysis was performed in a Perkin-Elmer Φ 5600-ci spectrometer using non-monochromatized Al K_α radiation (1486.6 eV). The sample analysis area was 800 μm in diameter and different spots were analysed in order to check for sample homogeneity. The standard deviation for the BEs values was ± 0.2 eV. Survey scans were obtained in the 0−1300 eV range (187.8 eV pass energy, 0.4 eV $step^{-1}$, 0.05 sec $step^{-1}$). Detailed scans were recorded for the C1s, O1s, Zr3d, N1s and Ce3d regions (23.5 eV pass energy, 0.1 eV $step^{-1}$, 0.1 sec $step^{-1}$). The experimental uncertainty on the reported atomic composition values does not exceed ± 5%. The XPS spectrometer was calibrated by assuming the binding energy (BE) of the Au $4f_{7/2}$ line at 83.9 eV with respect to the Fermi level. The BE shifts were corrected by assigning to the C1s peak associated with adventitious hydrocarbons a value of 284.8 eV.[3] Samples were mounted on steel holders and introduced directly in the fast-entry lock system of the XPS analytical chamber. The analysis involved Shirley-type background subtraction, non-linear least-squares curve fitting adopting Gaussian-Lorentzian peak shapes, and peak area determination by integration.[4] The atomic compositions were evaluated from peak areas using sensitivity factors supplied by Perkin-Elmer, taking into account the geometric configuration of the apparatus.[5]

HRTEM analysis was performed with a JEOL 2010F microscope equipped with a field emission gun. The point-to-point resolution of the instrument was 0.19 nm and the resolution between lines was 0.14 nm. Samples were deposited from alcohol suspensions over grids with holey-carbon film.

S1.3 Catalytic tests

All catalytic tests were carried out on the aged catalyst. The two steps of the water-splitting thermal cycle were evaluated separately with two different methodologies. The O_2 release at 1300 °C in N_2 atmosphere was calculated as the weight loss recorded during an 80min isothermal test performed in a thermogravimetric analyzer (Q600-TA Instruments).

The H_2 produced by water splitting reaction was measured in a gas analyzer (Autochem 2100, Micromeritics) following the approach described below and reported elsewhere.[6]

The aged catalyst (50 mg) was previously oxidized in air flow at 800 °C for 10min and cooled down to room temperature to assure its full oxidation before each H_2/H_2O redox cycle. In a redox cycle the sample was first purged in argon, reduced under a 4.1v% H_2/N_2 flow (to obtain the same degree of reduction achieved with the endothermic reduction step in N_2), evacuated in Ar flow for 1h and then oxidized by pulses of water vapor (30 v% in Ar flow, 30cc min^{-1}) at 800 °C. H_2 production was measured with a thermal conductivity detector considering the outcome of the first twenty pulses. This procedure was repeated 6 times.

For sake of clarity the experimental approach has been summarized in the layout below.

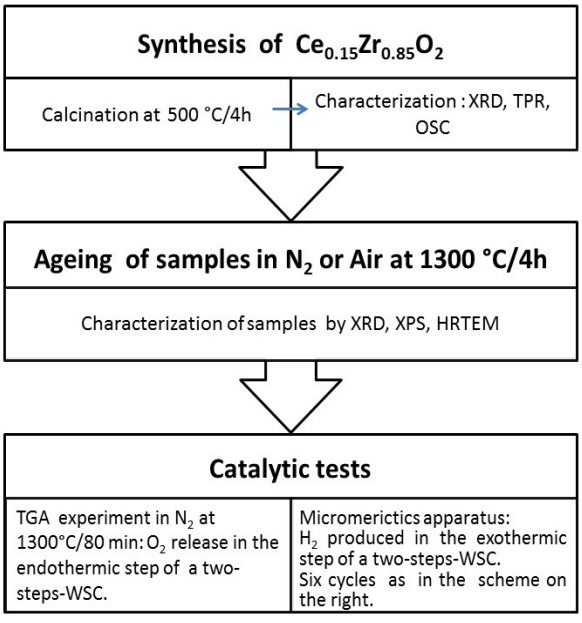

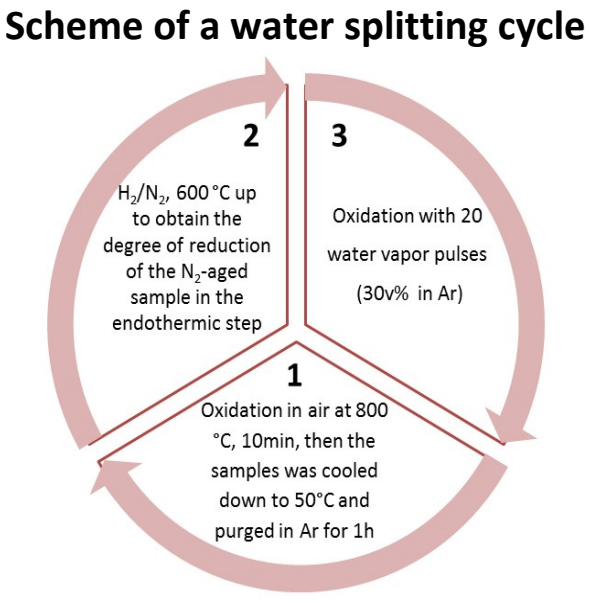

S2 Supplementary results

S2.1 Results related to fresh catalyst

The surface area of the fresh catalyst was 43 m^2/g and the OSC capacity was 850 μmol of O_2/g-CeO_2 at 650 °C. These values exceed those generally reported for similar compositions in the literature thanks to the beneficial effect of H_2O_2 and of surfactants treatment on the morphological characteristics of ceria based precipitates.[7]

Fig. S1 shows the TPR profile of the catalyst calcined at 500 °C in air. Redox behaviour of fresh catalyst is characterized by a single broad peak of hydrogen consumption in the 300-500 °C range, with a total H_2 uptake of 2.94 mmol/gCeO_2, corresponding to a Ce^{3+}/Ce_{tot} reduction degree of 84%. This is in line with results reported for samples of similar composition,[8] and suggest the formation of homogeneous solid solution.

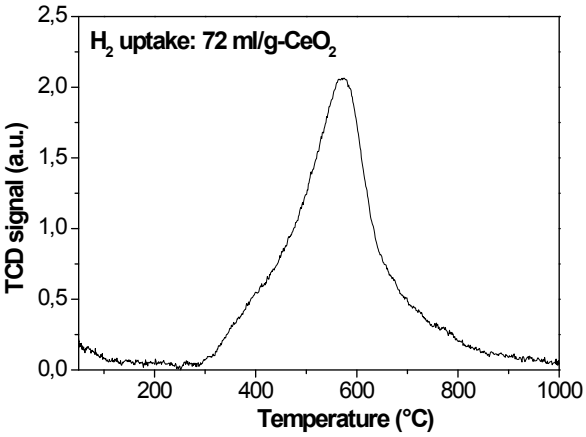

Fig. S1: TPR profile of fresh sample

S2.2 Results related to the aged catalyst

S2.2.1 HRTEM Characterization

Fig. S2 shows a HRTEM image of the sample treated in N_2 at 1300 °C where FT pattern is attributable to a CZ supercell. An enlargement of the area enclosed in the white square is shown in the inset, where the existence of the supercell is visible directly in the HRTEM image.

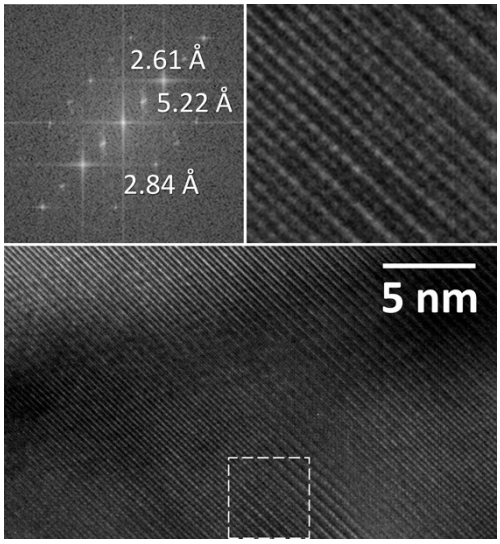

Fig. S2: HRTEM image of the sample treated in N_2 at 1300 °C.

Fig. S3 shows a HRTEM image of a sample after six redox cycles. No segregated phases are detectable due to the significant growth of particles whose size goes beyond the limit of HRTEM analysis.

Fig. S3: HRTEM image of the sample treated in N_2 at 1300 °C after six redox cycles.

S2.2.2 XPS Characterization

Fig. S4 shows the XPS spectrum related to Ce3d region before (continuous line) and after (dotted line) the water splitting process. We observe similar features before and after the cycle suggesting that the electronic environment of cerium is almost the same. In particular, both spectra are composed of three doublets (v, u), (v", u") and (v"', u"') corresponding to the emission from the spin-orbit split $3d_{5/2}$ and $3d_{3/2}$ core levels.[9-11] They are assigned to the different 4f configurations in the photoemission final states of tetravalent Ce^{4+} ions in Ce compounds. The highest binding energy peaks, v"' and u"' respectively located at 898.6 and 916.8 eV, are due to the Ce $3d^9$ $4f^0$ $O2p^6$ final state. The lowest binding energy states v (882.7 eV), u (901.2 eV) and v" (888.9 eV), u" (907.7 eV) are respectively assigned to the Ce $3d^9$ $4f^2$ $O2p^4$ and Ce $3d^9$ $4f^1$ $O2p^5$ photoemission final states. The intense and well separated u"' satellite peak is a fingerprint of Ce(IV) oxidation states. Therefore, the interpretation of the Ce3d spectra accounts for the presence of the six-peak structure of Ce^{4+} species indicating that the surface of the sample thermally treated in nitrogen resulted oxidized after exposure to air.

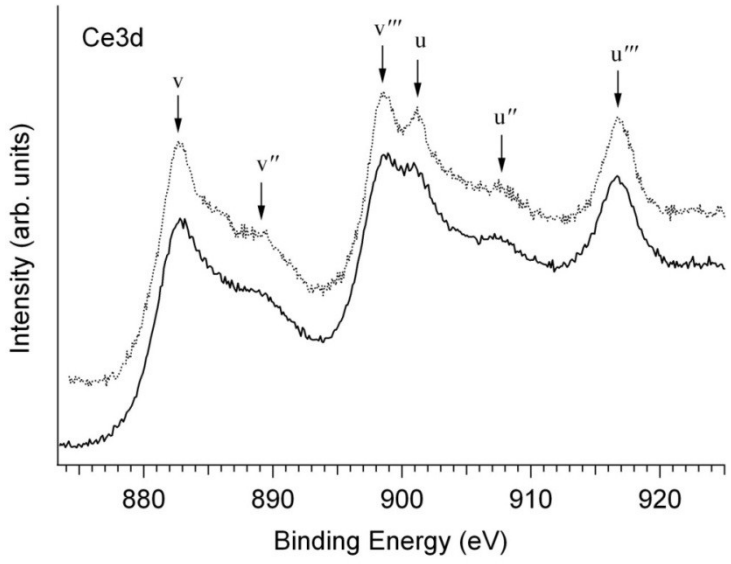

Fig. S4: High resolution XPS spectra of Ce3d region before (continuous lines) and after (dotted lines) the water splitting process.

In the sample, the measured BE for the $Zr3d_{5/2}$ line (182.1 eV) is characteristic for Zr(IV) ions in an oxide environment.[5]

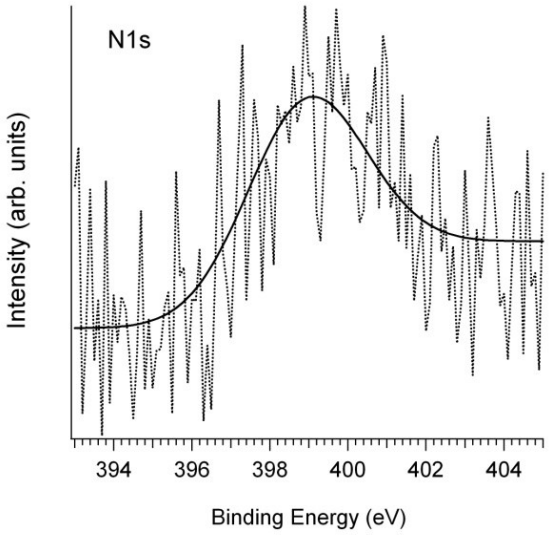

Fig. S5: N1s region recorded for the sample treated in N_2 flow at1300 °C for 4 hours.

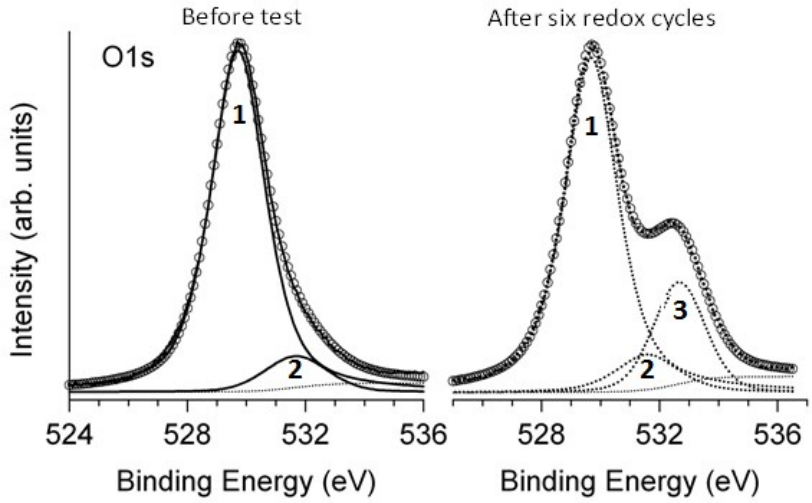

Fig. S6: O1s regions recorded for the sample treated in N_2 flow at 1300 °C for 4 hours before the water splitting test, and after six redox cycles. The fitting components of the O1s peaks are also reported: (1) oxygen in the oxide network,

(2) oxygen in the oxynitride phase, (3) adsorbed water molecules. Before the test, a small contribution of hydroxyl species to the component 2 cannot be excluded.

S2.2.3 Catalytic Results

The O_2 released from the sample treated in air during the endothermic step was 520 μmol/g-CeO_2. For a comparison between the water splitting activity of materials, the reduction degree of the air-treated sample in the H_2/H_2O redox cycles was set equal to that of the sample treated in N_2.

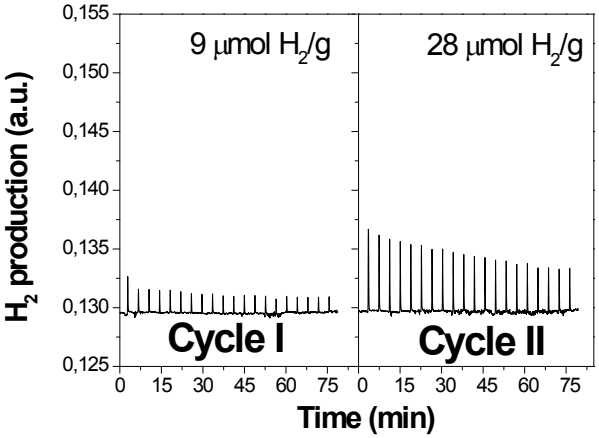

Fig. S7: H_2 production over two redox cycles at 800 °C of the sample treated in air at 1300 °C for 4 hours.

References

1 A.C. Larson and R.B. Von Dreele, *Laboratory report* LAUR (2000) pp. 86–748.

2 B.H. Toby, *J. Appl. Cryst*, 2001, **34**, 210.

3 D. Briggs and M. Seah, in *Practical Surface Analysis*, Ed. Wiley, Chichester, 1990.

4 D.A. Shirley, *Phys. Rev. B: Condens. Matter.,* 1972, **5**, 4709.

5 J.F. Moulder, W.F. Stickle, P.E. Sobol, K.D. Bomben, Handbook of X-ray Photoelectron Spectroscopy, Physical Electronics, J. Chastain (Ed.) Eden Prairie, MN, 1992.

6 N.D. Petkovich, S.G. Rudisill, L.J. Venstrom, D.B. Boman, J.H. Davidson and A. Stein, *J. Phys. Chem. C,* 2011, **115**, 21022.

7 A. Pappacena, P. Porreca, M. Boaro, C. de Leitenburg and A. Trovarelli, *Int. J. Hydrogen Energy*, 2011, **37**, 1698.

8 B. De Rivas, C. Sampedro, M. Garcia-Real, R. Lopez-Fonseca and J.I. Gutierrez-Ortiz, Appl. Catal. B: Env., 2013, **129**, 225.

9 A.E. Hughes, J.D. Gorrnan, P.J.K. Patterson and R. Carter, *Surf. Interface Anal.,* 1996, **24**, 634.

10 L. Armelao, D. Barreca, G. Bottaro, A. Gasparotto, E. Tondello, M. Ferroni and S. Polizzi., *Chem. Vapor Dep.,* 2004, **10**, 257.

11 E. Bêche, P. Charvin, D. Perarnau, S. Abanades and G. Flamant., *Surf. Interface Anal.,* 2008, **40**, 264.